

Magnetically tunable metallic photonic crystals immersed in liquid crystal for terahertz wave

Ru-Pin Pan^{*a}, Chih-Chang Shih^a, Tsung-Ta Tang^a, Yow-Gwo Wang^a,
Hsin-Ying Wu^a, Chia-Jen Lin^a, and Ci-Ling Pan^b

^a Dept. of Electrophysics, National Chiao Tung University, Hsinchu, Taiwan (ROC)

^b Department of Physics, National Tsing Hua University, Hsinchu, Taiwan (ROC)

ABSTRACT

We investigated the phenomena of a metallic photonic crystal (MPC) immersed in liquid crystal. According to our design, the photonic crystal has specific photonic band gap (PBG) and can be utilized as a filter. The device is filled with nematic liquid crystal (NLC), MDA-00-3461. The refractive indices of NLC can be magnetically controlled by reorienting the NLC molecules. Consequently, the corresponding PBG and the filtering performance of the device are tunable. According to our experimental results, the low frequency boundary of PBG at 0.121 THz can be blue shifted by 6.17 GHz, and the high frequency boundary of PBG at 0.175 THz can be shifted to the blue by 11.04 GHz. As a tunable THz filter, the peak transmittance at 0.187 THz can be blue shifted by 3.66 GHz.

Keywords: Liquid crystal, photonic crystal, Terahertz waves, magnetic field, metallic cylinders

1. INTRODUCTION

Photonic crystal (PC) is a material or device with periodically varied index of refraction. It has been intensively studied, because it can be used to control the propagation of light. Light propagating in PC is like the electrons in crystal; the photonic band gap (PBG) resulted and a band of light is forbidden to propagate in PC.¹ On the other hand, the terahertz wave (THz) technology has been advanced drastically in last decade. The THz wave has wavelength in the range between 30 and 3000 μm ; at this scale the size of devices are generally larger and easier to make, comparing those for visible light. Many research groups have successfully made 1-, 2-, and 3-dimensional PC using various methods for THz waves.²⁻⁵

In most of PC researches, once a PC is made, its optical properties are fixed. However, it is a desire to have PC with tunable properties. Liquid crystal is a versatile material; while some researches used its temperature effect to vary its index of refraction in PC,⁶⁻⁷ we have used the magnetic field to change the effective index of refraction in a metal plate with 2D hole arrays to vary the *enhanced emission* peak.⁸

In this work, 2-dimensional metallic photonic crystal (MPC) is made by arranging thin metallic needles to form a triangular lattice. This array is immersed in nematic liquid crystal (NLC) that can be reoriented by magnetic field. THz time domain spectroscopy technique is used to measure the transmission spectroscopy of this tunable MPC. In addition, Finite-difference time-domain (FDTD) simulation is used to obtain a theoretical transmission spectrum; the experimental results are compared with the simulation results.

In following sections, the method and results will be described and discussed in detail.

* rpchao@mail.nctu.edu.tw

2. METHODS

2.1 Experimental

The MPC sample consists of metallic cylinders, which are arranged periodically with triangular lattice structure. The metallic cylinders are nickel (Ni) coated straight hollow steel wires and the nominated diameter is $300\ \mu\text{m}$. The thickness of Ni coating is $100\pm 24\ \text{nm}$, which is roughly the same as the skin depth for THz wave. Therefore, the wires can be considered as a solid nickel cylinders in the following simulation.

To make the triangular arranged cylinders, a home-made template is used to arrange the cylinders first. Two sets of cylinders with diameter $300\ \mu\text{m}$ and $270\ \mu\text{m}$ are arranged alternately and touch each other to form a continuous plane. Then, the $300\ \mu\text{m}$ cylinders are removed, and the residual $270\ \mu\text{m}$ cylinders form a grid with regular spacing of $300\ \mu\text{m}$ between adjacent cylinders. A base is made by stacking three of the above grids with angle of 120° between each two layers as shown in Figure 1(a). Two identical bases, one on top and one on bottom, are put together to form a template. The $300\ \mu\text{m}$ cylinders are inserted through the holes of these two bases and the MPC with triangular lattice structure is then built. After some trimming work, the final MPC sample is as shown Figure 1(b). Each side is about 6mm. Two fused silica plates are glued to the two ends of the MPC sample. By using microscope to examine the MPC sample, we obtain the actual diameter d of cylinder being $286\pm 5\ \mu\text{m}$ and the lattice constant s being $642\ \mu\text{m}$.

The MPC sample is then put in a fused silica box and a NLC (MDA-00-3461 from Merck) is gradually filled into the box, one part at a time. After each filling, the sample is put in a vacuum chamber to pump out the air. When the box is finally filled up, a fused silica top is used to seal box. Now the liquid crystal immersed MPC sample is completed.

The NLC has positive magnetic anisotropy, and the applied magnetic field can rotate the director toward to the field direction. If the magnetic field is much larger than the threshold, we can roughly assume the director of all NLC molecules is parallel to the magnetic field. In this work a magnetic field of 800 gauss at sample position is used, while the threshold is about 250 gauss by considering the spacing between the cylinders.⁹ The magnetic field is supplied by a rare-earth magnet pair that is mounted on a rotational stage.

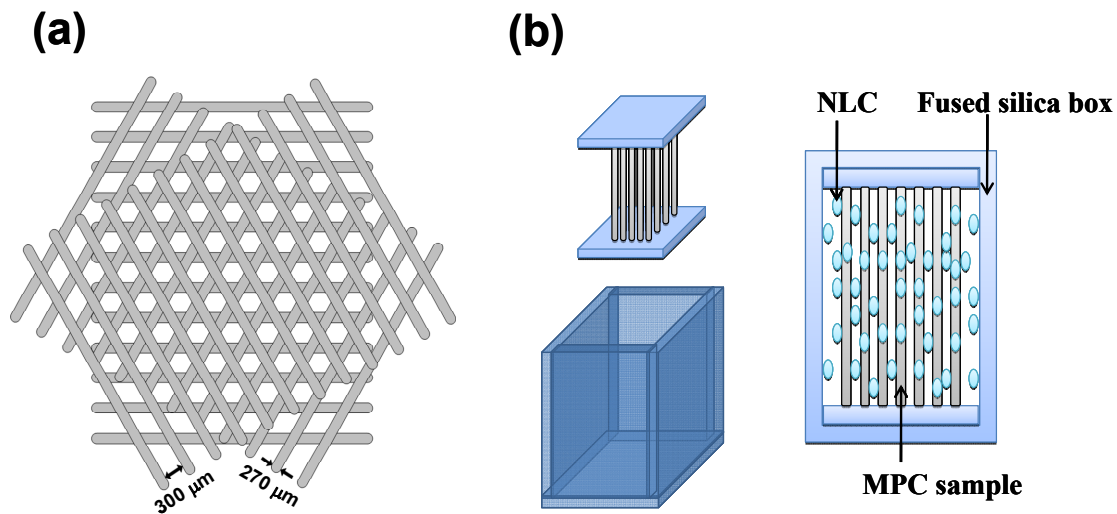


Figure 1. Sketch of the sample: (a) the template for making MPC, and (b) MPC in NLC.

The ordinary and extraordinary indices of refraction of the NLC in the THz range are 1.535 and 1.716, respectively.¹⁰ The effective index of refraction can be written as

$$n_{eff} = \left[\frac{\sin^2(\theta)}{n_o^2} + \frac{\cos^2(\theta)}{n_e^2} \right]^{-\frac{1}{2}}, \quad (1)$$

In our experiment, the θ value can be varied between 0° and 40° or set to be 90° ; n_{eff} then changes from n_e to n_o gradually with increasing θ .

The transmission spectrum is measured by using THz time domain spectroscopy as shown in Figure 2. The detail about the measurement has been describes in other works, for example, reference 8 and 10.

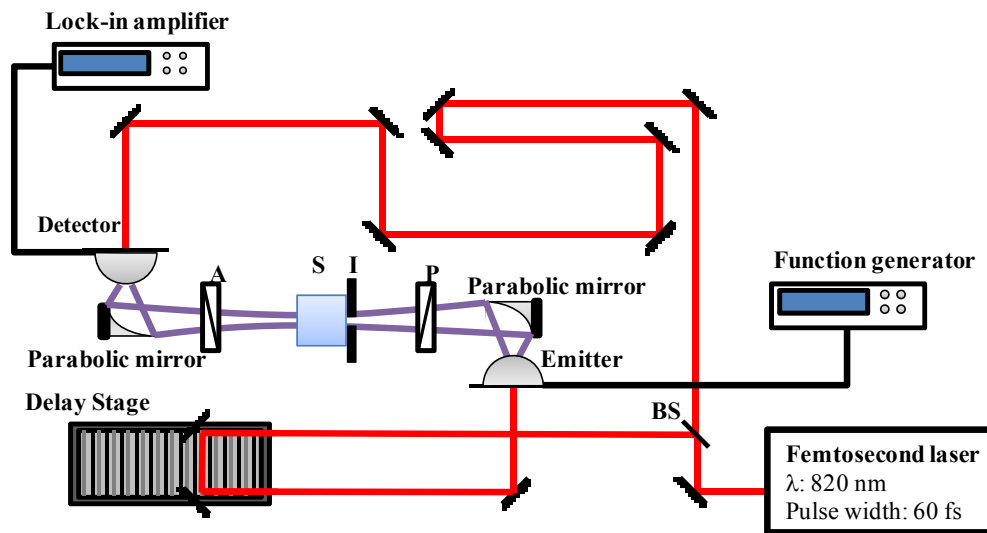


Figure 2. Sketch for THz-TDS. BS: Beam Splitter, P: Polarizer, A: Analyzer, S: Sample, and I: Iris.

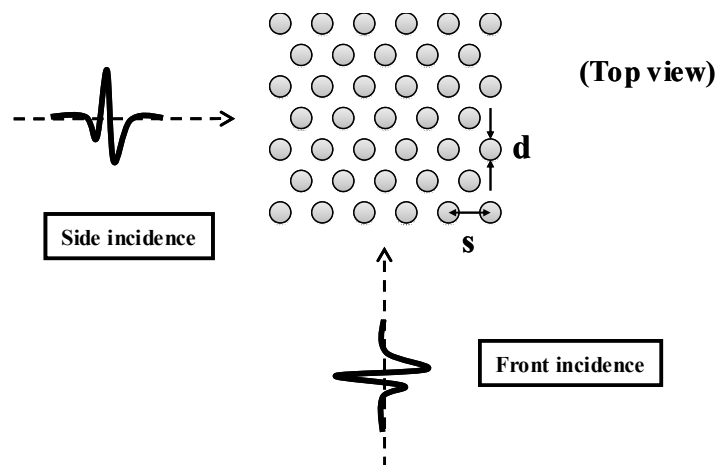


Figure 3. The geometry of incident THz waves with respect to the MPC.

The measurement setup is sketched in Figure 3; the THz waves are incident with two directions with respect to the MPC. One is called front incidence where light propagating perpendicular to the lattice vector. The other is called side

incidence where the wave propagating parallel to the lattice vector. The wave polarization is perpendicular to the MPC cylinders, i.e., parallel to the figure plane. The transmission spectrum of the empty fused silica box is measured and taken as a reference. The transmittance of the sample is relative to this reference.

2.2 Simulations

We have used the finite-difference time-domain (FDTD) method to simulate the wave propagating through the MPC, which can give us a comparison with our experimental data. It can also give us guidance for experimental conditions. In the simulation, the MPC is constructed with the real structure, only that the cylinders are considered as solid nickel cylinders. The index of refraction of nickel at THz range is taken as 463 at 0.3 THz. This value is calculated using the Drude dispersion model and parameters according to the work by Ordal et al.¹¹

Since both of the THz beam and the MPC are finite in size, the position for incidental position and beam size are important. In the simulation we can vary the beam size and the position of incidence, the *measuring point* is at a position after the MPC and facing the center of incident beam. In Figure 4 we show the scales used in our simulation, the two small rectangles indicate the *measuring points*, (321, 5000) and (-4400, 278), for the two incidence conditions, front and side incidence, respectively.

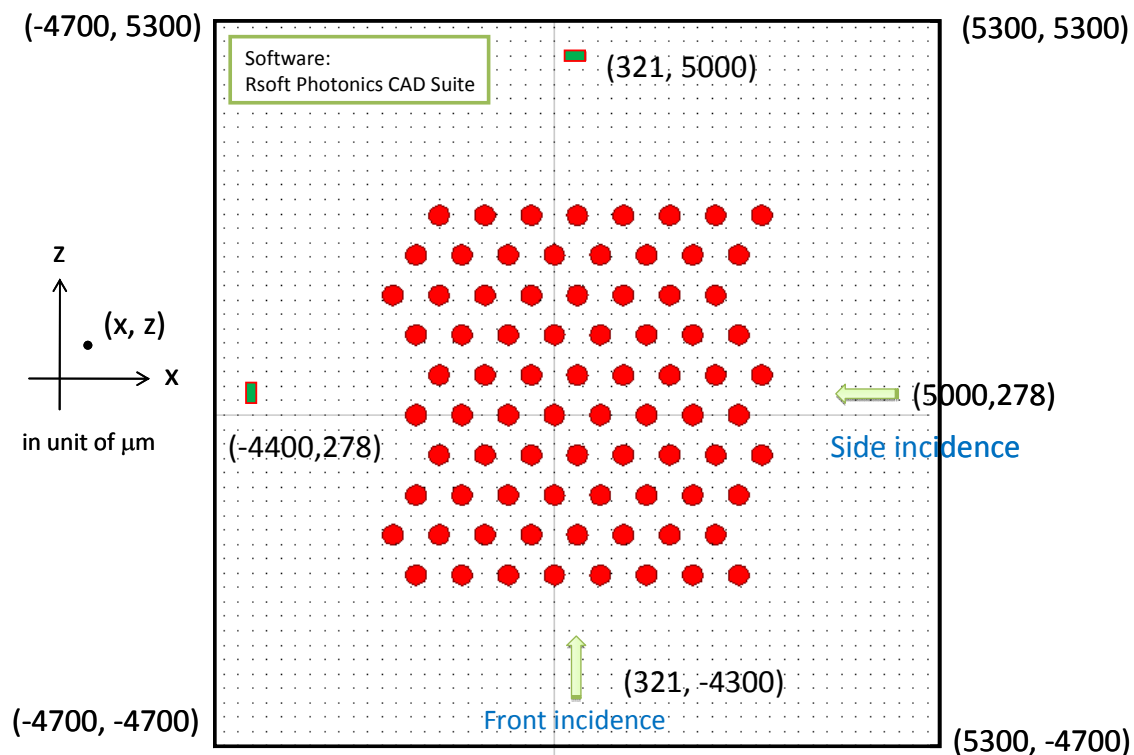


Figure 4. The positions used for simulation.

The incident beam has an intensity profile as

$$f(x, y, z_0) = e^{\left(-4\frac{x^2}{w^2}\right)} e^{\left(-4\frac{y^2}{w^2}\right)}, \quad (2)$$

where w is the beam diameter, which is adjusted according the beam size used in experiments.

3. RESULTS

Both of the experimental and simulated results for beam diameters between 3 and 9 mm and with front incidence are shown in Figure 5. There is a clear peak in each of the ranges of 0.3~0.5 THz and 0.5~0.7 THz. On the other hand, the range between 0.2 and 0.3 THz is like a photonic band gap. With increasing beam diameter, the transmittance decreases. Even when the beam size becomes larger than the MPC size, 6 mm, the transmittance does not increase with the diameters.

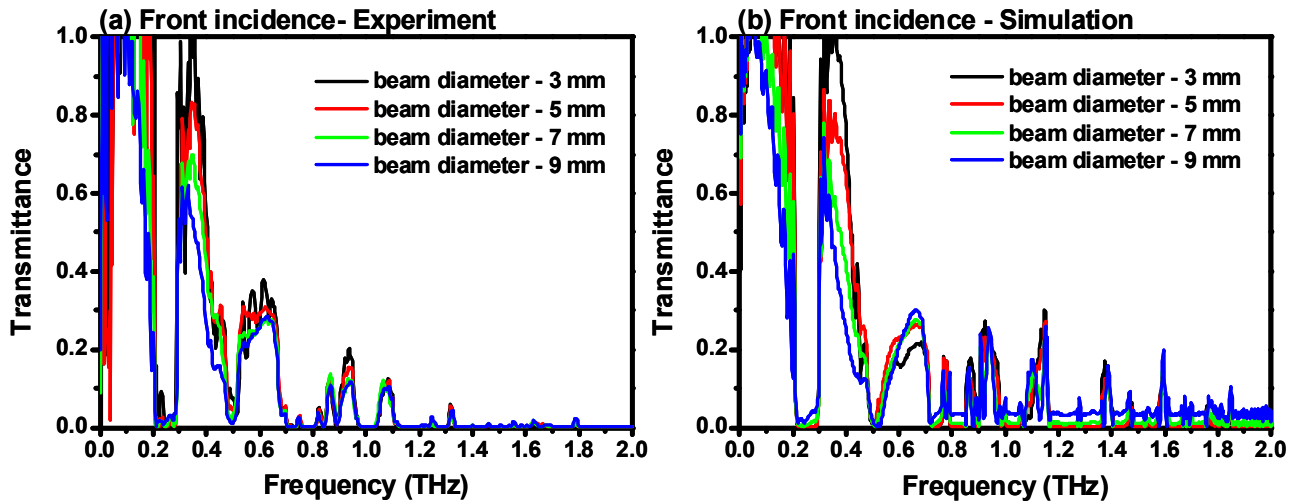


Figure 5. The beam size effect on the transmission spectrum of THz waves. (a) experiment and (b) simulation.

We also consider whether the incident point on the MPC is critical. The simulated results show that we can move the beam around the middle for a range of one lattice constant and the results are almost identical. Figure 6 shows the simulated results for the center of beam moving at 5 positions: A, B_R , B_L , C_R , C_L ; A is the geometrical center at the front face, B_R and B_L are 0.3 lattice constant away from the center at either side, while C_R and C_L are 0.5 lattice constant away from the center at each side. For a beam diameter of 5 mm, all of these five situations give almost identical transmittance. This results tells us that if we have the MPC centered at the beam path, an fluctuation of position under one lattice is negligible. From now on we fix our beam diameter at 5 mm for all measurements.

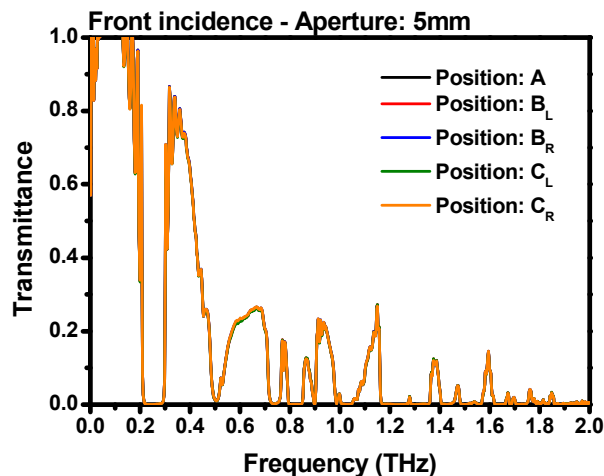


Figure 6. The incidence position effect on transmittance. The beam diameter is fixed at 5 mm.

In the experiments, the NLC orientations are varied by rotating the magnets, while in simulation the reorientation angle determines the effective index of refraction of NLC according to Eq.(1). In Figure 7, we show the measured spectrum and simulated spectrum for several reorientation angles. We can see that there is almost no transmitting for frequency higher than 0.4 THz; while a peak is clearly seen at frequency close to 0.2 THz. This peak frequency increases with the reorientation angle. However, the measured transmittance decreases with the increasing angle, although the simulated result does not show this decrease.

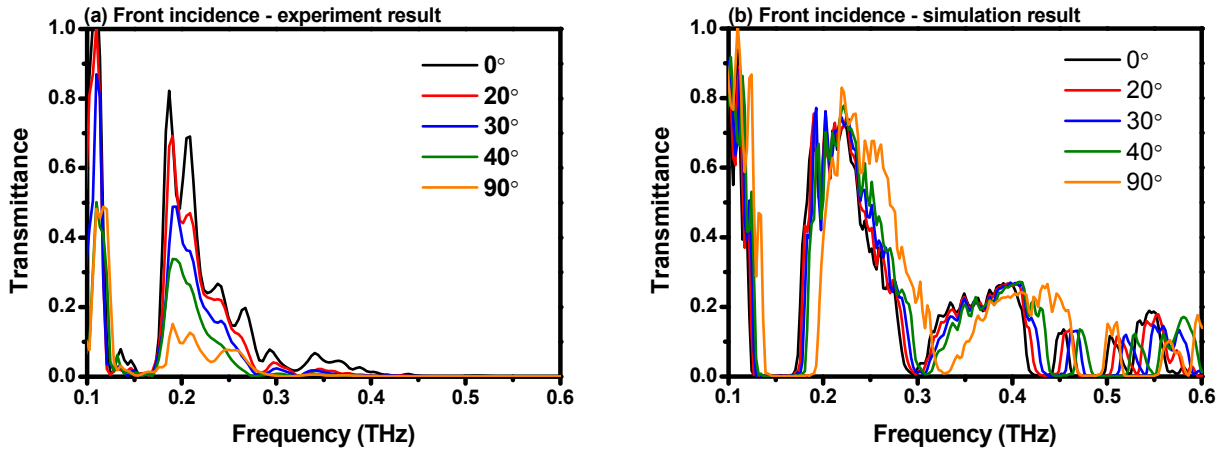


Figure 7. The transmission spectrum of liquid crystal immersed MPC at various magnetic field direction for front incidence. (a)experiment and (b) simulation.

For the peak at 0.2 THz, the positions of peaks are determined by fitting the curves with Gaussian function. Figure 8 shows the relation between the position of fitted peak and the effective index of refraction calculated by using Eq. (1). The peak positions shift to lower frequency when the effective index of refraction moves from n_o (1.535) to n_e (1.716). The theoretical curve and experimental curves show same trend, except that the tunable range in experiments is smaller than the theoretically predicted range.

To analyze the band gap shown in Figure 7, we define the gap edge being the frequencies with transmittance becomes smaller than 0.1. The relations between the band gap edges and the effective index of refraction are shown in Figure 9. The beginning and ending frequencies of the gap from both experiment and simulation are plotted; they agree with each other closely. The experimental shift is 6.17 GHz for lower edge and 11.04 GHz for higher edge.

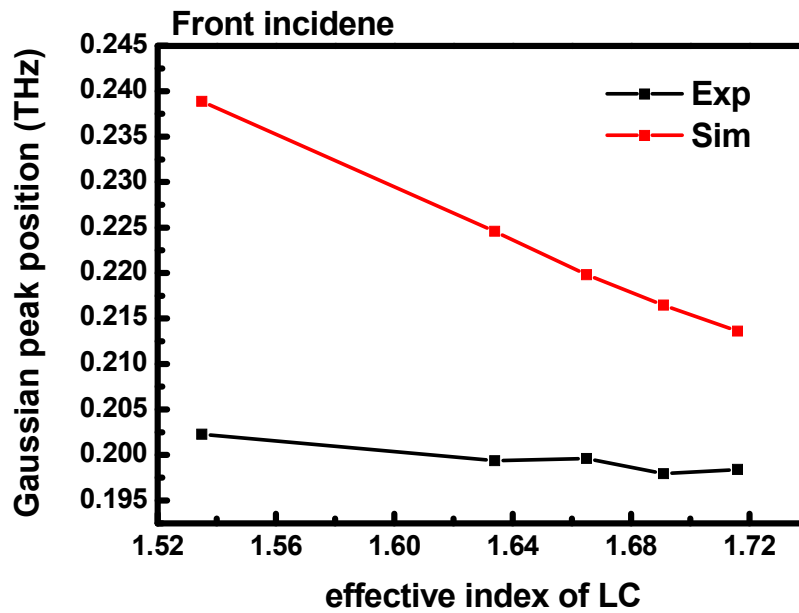


Figure 8. The peak positions vs. effective index of refraction.

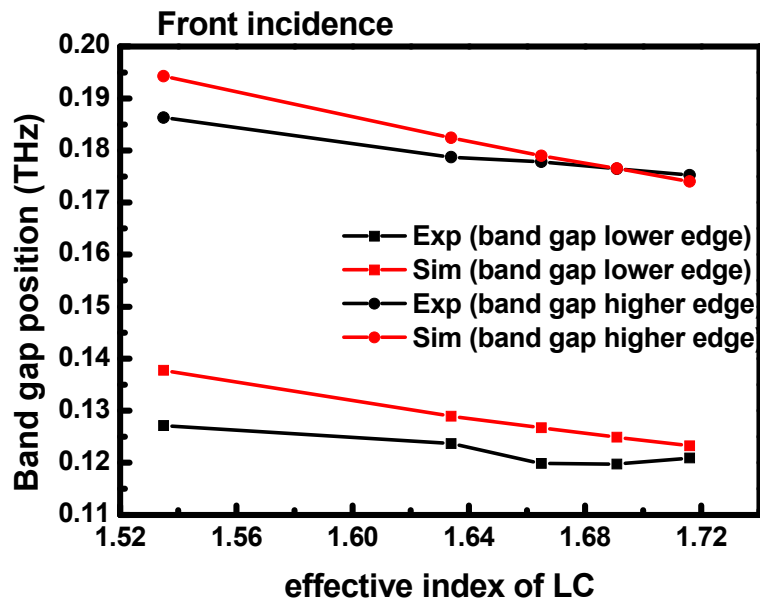


Figure 9. The band gap positions vs. the effective index of refraction.

4. CONCLUSION

We have made a metallic photonic crystal (MPC), which is shown having tunable band gap and peak transmission frequency for THz waves. This MPC is immersed in nematic liquid crystal and the controlling is done by applying a

magnetic field that can rotate and thus reorient the liquid crystal molecules. The lower edge of band gap shifts from 0.121 THz to 0.127 THz while the higher edge shifts from 0.175 THz to 0.186 THz as the effective index of refraction changes due to the molecular reorientation. As a tunable filter, the peak position is at 0.187 THz and the controllable range is 3.66 GHz. The insertion loss is between 0.85 db and 7.2 dB.

Acknowledgements

This work was partially supported by National Science Council, Republic of China, under grant 96 -2221- E- 009 -131 -MY3.

REFERENCES

- [1]. Sajeev John, "Strong Localization of Photons in Certain Disordered Dielectric Superlattices," *Phys. Rev. Lett.*, **58**, 2486-2489 (1987)
- [2]. E. Özbay, E. Michel, G. Tuttle, R. Biswas, M. Sigalas, and K.-M. Ho, "Micromachined millimeter-wave photonic band-gap crystals," *Appl. Phys. Lett.*, **64**, 2059-2061 (1994).
- [3]. E. Özbay, E. Michel, G. Tuttle, R. Biswas, K. M. Ho, J. Bostak, and D. M. Bloom "Terahertz spectroscopy of three-dimensional photonic band-gap crystals," *Optics Letters*, **19**, 1155-1157 (1994).
- [4]. Shao-Wei Wang, Wei Lu, Xiao-Shuang Chen, Zhi-Feng Li, Xue-Chu Shen, and Weijia Wen, "Two-dimensional photonic crystal at THz frequencies constructed by metal-coated cylinders," *J. Appl. Phys.*, **93**, 9401-9403 (2003).
- [5]. Fumiaki Miyamaru and Masanori Hangyo, "Polarization response of two-dimensional metallic photonic crystals studied by terahertz time-domain spectroscopy," *Applied Optics*, **43**, 1412-1415 (2004).
- [6]. S. W. Leonard, J. P. Mondia, H. M. van Driel, O. Toader, S. John, K. Busch, A. Birner, U. Gösele, and V. Lehmann., "Tunable two-dimensional photonic crystals using liquid-crystal infiltration," *Phys. Rev. B*, **61**, 2389-2392 (2000).
- [7]. Chul-Sik Kee, H. Lim, Young-Ki Ha, Jae-Eun Kim, and Hae Yong Park, "Two-dimensional tunable metallic photonic crystals infiltrated with liquid crystals," *Phys. Rev. B*, **64**, 085114, (2001).
- [8]. Ci-Ling Pan, Cho-Fan Hsieh, Ru-Pin Pan, Masaki Tanaka, Fumiaki Miyamaru, Masahiko Tani, and Masanori Hangyo "Control of enhanced THz transmission through metallic hole arrays using nematic liquid crystal," *Optics Express*, **13**, 3921-3930 (2005).
- [9]. P. G. De Gennes and J. Prost, *The Physics of Liquid Crystals*, **2nd ed.**, (Oxford, New York, 1993).
- [10]. Cheng-Pin Ku, Chih-Chang Shih, Chia-Jen Lin, Ru-Pin Pan, Ci-Ling Pan "THz Optical Constants of the Liquid Crystal MDA-00-3461" *Mol. Cryst. Liq. Cryst.*, Vol. 541: pp. 65/[303]-70/[308], Jun 30 2011.
- [11]. M. A. Ordal, Robert J. Bell, R. W. Alexander, Jr. L. L. Long, and M. R. Querry, "Optical properties of fourteen metals in the infrared and far infrared: Al, Co, Cu, Au, Fe, Pb, Mo, Ni, Pd, Pt, Ag, Ti, V, and W," *Appl. Optics*, **24**, 4493-4499(1985).